Struct Multidisc Optim (2010) 40:353–364
DOI 10.1007/s00158-009-0374-4

RESEARCH PAPER

Shape sensitivity analysis with design-dependent loadings—equivalence between continuum and discrete derivatives

Jalal Akbari · Nam H. Kim · M. T. Ahmadi

Received: 24 May 2009 / Accepted: 31 May 2009 / Published online: 10 June 2009

Abstract The purpose of this paper is twofold: (1) showing equivalence between continuum and discrete formulations in sensitivity analysis when a linear velocity field is used and (2) presenting shape sensitivity formulations for design-dependent loadings. The equations for structural analysis are often composed of the stiffness part and the applied loading part. The shape sensitivity formulations for the stiffness part were well-developed in the literature, but not for the loading part, especially for body forces and surface tractions. The applied loads are often assumed to be conservative or design-independent. In shape design problems, however, the applied loads are often functions of design variables. In this paper, shape sensitivity formulations are presented when the body forces and surface tractions depend on shape design variables. Especially, the continuum–discrete (C–D) and discrete–discrete (D–D) approaches are compared in detail. It is shown that the two methods are theoretically and numerically equivalent when the same discretization, numerical integration, and linear design velocity fields are used. The accuracy of sensitivity calculation is demonstrated using a cantilevered beam under uniform pressure and an arch dam crown cantilever under gravity and hydrostatic loading at the upstream face of the structure. It is shown that the sensitivity results are consistent with finite difference results, but different from the analytical sensitivity due to discretization and approximation errors of numerical analysis.

Keywords Shape optimization · Shape sensitivity · Continuum sensitivity · Discrete sensitivity · Design-dependent loading

1 Introduction

In structural sensitivity analysis, there are currently four broad categories of methods in common use for obtaining the derivatives of performance measures with respect to design variables (van Keulen et al. 2005): (a) global finite differences, (b) discrete derivatives, (c) continuum derivatives, and (d) computational or automatic differentiation. The choice between the different options for calculating derivatives is influenced by three criteria: accuracy, computational cost and implementation effort. Since the global finite difference and computational differentiation are a black-box type approach, they do not require much knowledge on structural analysis. However, the discrete and continuum derivatives require understanding the structural analysis procedure and differentiating the system of

J. Akbari · N. H. Kim
University of Florida, Gainesville, FL 32611, USA
e-mail: akbari@malayeru.ac.ir

N. H. Kim (✉)
Department of Mechanical & Aerospace Engineering,
University of Florida, Gainesville, FL 32611, USA
e-mail: nkim@ufl.edu

M. T. Ahmadi
Department of Civil Engineering,
Tarbiat Modares University, Tehran, Iran
e-mail: mahmadi@modares.ac.ir

Present Address:
J. Akbari
Faculty of Civil Engineering, Department of Engineering,
Malayer University, Malayer, Iran

equations. The difference between these two approaches is when the structural equations are differentiated with respect to the design variables. The discrete method (Haftka and Adelman 1989; Kwak 1994) differentiates the system of equations after discretization, while the continuum method (Arora 1993; Arora et al. 1992; Choi and Kim 2004) differentiates the continuum equation first followed by discretization. The difference between these two methods is particularly important for shape design problems, because the shape design variables change the discretization, i.e., mesh or grid. The discussion for selecting appropriate sensitivity calculation method can be found in the literature, including possibility of using different numerical methods (Haftka and Grandhi 1986; Mota Soares et al. 1984; Santos and Choi 1989) and possibility of implementing outside of finite element analysis programs using postprocessing data (Arora et al. 1992; Mota Soares et al. 1984; Santos and Choi 1989).

Several comparisons between the continuum and discrete methods have been conducted in the literature (Haftka and Adelman 1989; Yang and Botkin 1986; Choi and Twu 1988). Especially, Choi and Twu (1988) showed that both methods are equivalent when they have (1) same discretization (shape function), (2) exact integration (not numerical integration), (3) analytical (not numerical) finite element solutions, and (4) linear velocity field and consistent mesh perturbation. It was shown that the sensitivity results of both methods are different when quadratic and cubic design velocity fields are used. In the practical point of view, the requirements in (1) and (4) are reasonable, but the requirements in (2) and (3) can be significant. Most sensitivity calculations use the same finite element model with linear velocity field. Although nonlinear mesh perturbation can sometimes reduce mesh distortion (especially when it is integrated with solid models (Hardee et al. 1999)), a consistent mesh perturbation with design velocity field is popular due to its simplicity. However, most finite element programs use numerical integration and calculate numerical solutions. The reason for these two requirements is that Choi and Twu (1988) tried to remove any numerical errors in their comparison. The objective of this paper is to show that these two requirements are unnecessary, and the two formulations are equivalent in the discrete level. In fact, this paper is the first one that shows the equivalence of the two methods in the discrete level. Thus, as long as the same numerical integration method and matrix equation solver are used, the same sensitivity results are expected. However, it is noted that the results of the two methods are still different when nonlinear velocity fields are used.

In many complex problems, it is impractical to solve the sensitivity equations analytically. Numerical methods, such as finite element analysis, are employed to solve the sensitivity equations. Thus, it is appropriate that the comparison between sensitivity methods is performed in the discrete level. When both discrete and continuum methods calculate sensitivity using numerical methods, the former will be called a discrete–discrete (D–D) method, while the latter a continuum–discrete (C–D) method (Choi and Twu 1988).

Most comparisons in the previous studies were focused on the stiffness part. The applied loads are often assumed to be conservative or design-independent. In this paper, shape sensitivity formulations are presented when body forces and surface tractions depend on the shape design variables. We showed that the final sensitivity expressions for both methods are identical if the same circumstances are applied. First, the same discretization must be used for finite element analysis. Second, the same numerical integration method must be carried out for all terms such as stiffness and loading parts in two approaches. The last condition is that movement of finite element grid points for shape design change in discrete method must be consistent with the parameterization method used for the linear design velocity field of continuum method.

2 Structural equations for linear elasticity

In this section, the structural equation for three-dimensional linear elasticity is introduced followed by discretization using the finite element method and numerical integration using Gauss quadrature. This section is necessary for the following sensitivity derivations.

Let $\bar{\mathbf{z}}$ be the displacement variation and $\mathbb{Z}$ the space of kinematically admissible displacements that satisfy homogeneous, essential boundary conditions (Hughes 1987). For given body force $\mathbf{b}$ and surface traction $\mathbf{t}$, the weak form of the structural equation in the continuum domain Ω is to find displacement field $\mathbf{z}$ that satisfies:

$$a_\Omega(\mathbf{z},\bar{\mathbf{z}}) \equiv \iiint_\Omega \varepsilon(\bar{\mathbf{z}})^T \mathbf{C}\varepsilon(\mathbf{z})\, d\Omega = \iiint_\Omega \bar{\mathbf{z}}^T \mathbf{b}\, d\Omega + \iint_{\Gamma_s} \bar{\mathbf{z}}^T \mathbf{t} d\Gamma \equiv \ell_\Omega(\bar{\mathbf{z}}), \quad \forall\, \bar{\mathbf{z}} \in Z \tag{1}$$

where $\varepsilon(\mathbf{z})$ is the engineering strain vector, $\mathbf{C}$ is the elasticity matrix, and Γ_s is the traction boundary. In this paper, the superposed "–" denotes the variation of a quantity. For notational convenience, the forms

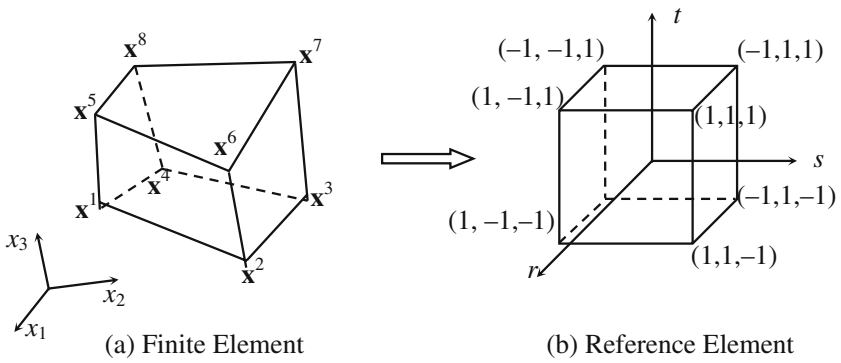

(a) Finite Element (b) Reference Element

Fig. 1 Isoparametric, eight-node hexahedron element

$a_\Omega(\mathbf{z}, \bar{\mathbf{z}})$ and $\ell_\Omega(\bar{\mathbf{z}})$ are used for structural energy and external load, respectively.

In order to solve the structural equation (1) in general, it is first discretized by finite elements and then integrated using numerical integration. We will briefly illustrate the numerical integration of a single element. For more detailed explanation, the readers are referred to Hughes (1987). Consider an isoparametric, eight-node hexahedral element in Fig. 1 in the physical and reference domains. In the finite element, the displacement is approximated using nodal displacements and shape functions as

$$\mathbf{z}(r, s, t) = \mathbf{N}(r, s, t) \cdot \mathbf{d} \tag{2}$$

where $\mathbf{N}(r, s, t)$ is the matrix of shape functions and $\mathbf{d}$ is the vector of nodal displacements. In the Galerkin approximation, the displacement variation, $\bar{\mathbf{z}}$, is approximated using the same shape function with displacement; i.e., $\bar{\mathbf{z}} = \mathbf{N} \cdot \bar{\mathbf{d}}$ with $\bar{\mathbf{d}}$ being the nodal displacement variation. In addition, the vector of strains in (1) can also be obtained by differentiating the displacement with respect to spatial coordinates as

$$\varepsilon(\mathbf{z}) = \mathbf{B} \cdot \mathbf{d} \tag{3}$$

where $\mathbf{B}$ is the strain–displacement matrix. Note that the shape function in (2) is independent of shape design because it is defined in the reference domain, while the strain-displacement matrix depends on the shape design because it contains the derivative with respect to the spatial coordinates.

In this paper, we only consider numerical integration using Gauss quadrature. For a single element, the discretized structural energy form becomes

$$a_\Omega(\mathbf{z}, \bar{\mathbf{z}}) \cong \bar{\mathbf{d}}^T \left[\sum_{i=1}^{N_{\text{quad}}} w_i \left(\mathbf{B}^T \mathbf{C} \mathbf{B} \right)_{(i)} \left| \mathbf{J}_{(i)} \right| \right] \mathbf{d} = \bar{\mathbf{d}}^T \mathbf{K} \mathbf{d} \tag{4}$$

where N_{quad} is the number of integration points, w_i is the integration weight, $\mathbf{J} = \left[\partial \mathbf{x} / \partial \mathbf{r} \right]$ is the Jacobian relation between the physical and reference element, and $\mathbf{K}$ is the element stiffness matrix. The subscribed (i) is the value of the function at the particular integration point. The discretization of the load form will be discussed in Sections 5.2 and 5.3.

3 Shape design parameterization and design velocity field

In shape design, the shape of the domain that a structural component occupies is treated as a design variable. Suppose that the initial structural domain Ω with boundary Γ is changed into the perturbed domain Ω_τ with boundary Γ_τ in which the parameter τ controls the amount of shape perturbation (see Fig. 2). By defining the design changing direction to be $\mathbf{V}(\mathbf{x})$, the material point at the perturbed design can be denoted as $\mathbf{x}_\tau = \mathbf{x} + \tau \mathbf{V}(\mathbf{x})$. Since the shape changing process is similar to the dynamic process with τ being time, the design changing direction, $\mathbf{V}(\mathbf{x})$, is called a design velocity. Since every shape design variable changes domain, it must be represented by a design velocity field. In the following derivations, we will consider a single shape design variable.

It is important to understand the relation between the shape design variable and the design velocity field. In addition, as the sensitivity equation is going to

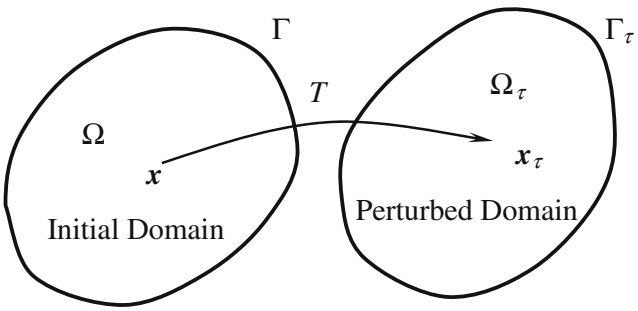

Fig. 2 Variation of domain according to shape change

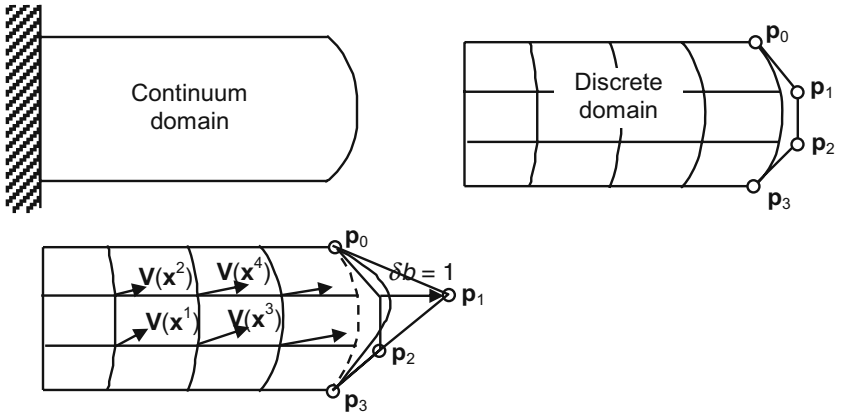

Fig. 3 Shape design variable and the corresponding design velocity vector at discrete domain

be solved numerically in the discrete domain, it is necessary to obtain the discrete design velocity from the above continuous design velocity field, $\mathbf{V}(\mathbf{x})$. As an illustration, consider a two-dimensional domain in Fig. 3 whose boundary is parameterized using parametric curves. A shape design variable is defined such that control point $\mathbf{p}_1$ moves in the horizontal direction. As the domain is changed according to the shape design variable, the locations of nodes will also be changed. The direction of coordinate change of each node is defined as a discrete design velocity vector. For the purpose of comparison, this paper assumes that both the continuum and discrete methods use the same linear, discrete design velocity vector.

4 Shape design sensitivity equation—continuum derivatives

4.1 Material derivative formulas

In the continuum theory of design sensitivity analysis, the solution $\mathbf{z}_\tau(\mathbf{x}_\tau)$ of structural problems at the perturbed shape is assumed to be a differentiable function with respect to the shape design variable. Then, the total change in the solution is composed of the change at the fixed location (partial derivative) and the change caused by movement of the material point. Since this is similar to the material derivative concept in continuum mechanics, the terms material derivative has been adopted for shape sensitivity (Choi and Haug 1983). The material derivative of $\mathbf{z}_\tau(\mathbf{x}_\tau)$ at $\mathbf{x} \in \Omega$ is defined as

$$\dot{\mathbf{z}} = \lim_{\tau \to 0} \frac{\mathbf{z}_\tau(\mathbf{x} + \tau \mathbf{V}(\mathbf{x})) - \mathbf{z}(\mathbf{x})}{\tau} \tag{5}$$

which is the rate of change in displacement as the shape of the domain is perturbed in the direction of $\mathbf{V}(\mathbf{x})$. Note that in a strict sense the material derivative in (5) is the variation of function $\mathbf{z}_\tau(\mathbf{x}_\tau)$ in the direction of $\mathbf{V}(\mathbf{x})$ (Choi and Kim 2004). If the variation of a function is continuous and linear with respect to $\mathbf{V}(\mathbf{x})$, then the function is differentiable. For rigorous discussion of differentiability, refer to Haug et al. (1985).

Useful formulas for deriving sensitivity expressions are presented first. The Jacobian relation between the initial and perturbed design can be written as

$$\mathbf{T} = \frac{\partial \mathbf{x}_\tau}{\partial \mathbf{x}} = \mathbf{I} + \tau \frac{\partial \mathbf{V}}{\partial \mathbf{x}} = \mathbf{I} + \tau \nabla \mathbf{V} \tag{6}$$

Note that the above Jacobian $\mathbf{T}$ should not be confused with the Jacobian $\mathbf{J}$ between the physical and reference domains in finite element discretization. The material derivative of the Jacobian and that of the determinant can be obtained as (Choi and Kim 2004)

$$\frac{d}{d\tau}(\mathbf{T})\bigg|_{\tau=0} = \nabla \mathbf{V} \tag{7}$$

$$\frac{d}{d\tau}|\mathbf{T}|\bigg|_{\tau=0} = div\mathbf{V} \tag{8}$$

The design sensitivity equation is obtained by differentiating the structural equation (1). The derivative of the energy form then becomes

$$\frac{d}{d\tau} a_{\Omega_\tau}(\mathbf{z}_\tau, \bar{\mathbf{z}}_\tau)\bigg|_{\tau=0} = a_\Omega(\dot{\mathbf{z}}, \bar{\mathbf{z}}) + a'_{\mathbf{V}}(\mathbf{z}, \bar{\mathbf{z}}) \tag{9}$$

The first term on the right-hand side represents implicit dependence on the design through the field variable, $\mathbf{z}$, while the second term, the structural fictitious load, denotes explicit dependence on the design velocity

$\mathbf{V}(\mathbf{x})$. In a similar way, the derivative of the load form becomes

$$\frac{d}{d\tau}\ell_{\Omega_\tau}(\bar{\mathbf{z}}_\tau)\bigg|_{\tau=0} = \ell'_{\mathbf{V}}(\bar{\mathbf{z}}) \tag{10}$$

Note that there is no implicitly dependent term in the derivative of the load form because all applied loads are explicitly dependent on the design variable. Detailed expressions of $a'_{\mathbf{V}}(\mathbf{z},\bar{\mathbf{z}})$ and $\ell'_{\mathbf{V}}(\mathbf{z})$ will be presented in the following subsections.

Using (9) and (10), the design sensitivity equation is obtained as

$$a_\Omega(\dot{\mathbf{z}},\bar{\mathbf{z}}) = \ell'_{\mathbf{V}}(\bar{\mathbf{z}}) - a'_{\mathbf{V}}(\mathbf{z},\bar{\mathbf{z}}), \quad \forall\,\bar{\mathbf{z}}\in Z \tag{11}$$

Note that by substituting $\dot{\mathbf{z}}$ into $\mathbf{z}$, the left-hand side of the design sensitivity equation (11) takes the same form as that of the structural analysis in (1). Thus, the same stiffness matrix can be used for sensitivity analysis and structural analysis, with different right-hand sides.

4.2 Energy form

The explicitly dependent term in (9) is a linear function of design velocity, given in (Kim et al. 2003)

$$a'_{\mathbf{V}}(\mathbf{z},\bar{\mathbf{z}}) = \iint_\Omega \Big[\varepsilon_{\mathbf{V}}(\bar{\mathbf{z}})^T\mathbf{C}\varepsilon(\mathbf{z}) + \varepsilon(\bar{\mathbf{z}})^T\mathbf{C}\varepsilon_{\mathbf{V}}(\mathbf{z}) + \varepsilon(\bar{\mathbf{z}})^T\mathbf{C}\varepsilon(\mathbf{z})\, div\mathbf{V}\Big]\, d\Omega \tag{12}$$

where $\varepsilon_{\mathbf{V}}(\mathbf{z})$ is the explicitly dependent term of $\varepsilon(\mathbf{z})$ on design velocity $\mathbf{V}(\mathbf{x})$. In (12), $div\mathbf{V} = \partial V_i/\partial x_i$ is the divergence of the design velocity, and $\nabla\mathbf{V} = \left[\partial V_i/\partial x_j\right]$ is the gradient matrix of the design velocity.

The structural fictitious load in (12) can be approximated using the same finite element discretization with the structural equation. First, the design velocity field, $\mathbf{V}(\mathbf{x})$, should be discretized. Let us assume that the discrete design velocity vector is available at each node. Then, the divergence of the design velocity can be obtained using the derivative of shape functions as

$$div\mathbf{V} = \sum_{i=1}^{3} V_{i,i} = \sum_{k=1}^{8}\left(N_{k,1}V_1^k + N_{k,2}V_2^k + +N_{k,3}V_3^k\right) \tag{13}$$

where $N_{k,i} = \partial N_k/\partial x_i$ is the spatial derivative of the shape function and V_i^k is the i-th component of design velocity at k-th node. Note that we use linear design velocity field; i.e., the design velocity varies linearly within the element. The gradient matrix of the design velocity can be obtained using a similar way, as

$$\begin{aligned}[\nabla\mathbf{V}] &= \begin{bmatrix} \frac{\partial V_1}{\partial x_1} & \frac{\partial V_1}{\partial x_2} & \frac{\partial V_1}{\partial x_3} \\ \frac{\partial V_2}{\partial x_1} & \frac{\partial V_2}{\partial x_2} & \frac{\partial V_2}{\partial x_3} \\ \frac{\partial V_3}{\partial x_1} & \frac{\partial V_3}{\partial x_2} & \frac{\partial V_3}{\partial x_3} \end{bmatrix} \\ &= \begin{bmatrix} \frac{\partial V_1}{\partial r} & \frac{\partial V_1}{\partial s} & \frac{\partial V_1}{\partial t} \\ \frac{\partial V_2}{\partial r} & \frac{\partial V_2}{\partial s} & \frac{\partial V_2}{\partial t} \\ \frac{\partial V_3}{\partial r} & \frac{\partial V_3}{\partial s} & \frac{\partial V_3}{\partial t} \end{bmatrix} \begin{bmatrix} \frac{\partial r}{\partial x_1} & \frac{\partial r}{\partial x_2} & \frac{\partial r}{\partial x_3} \\ \frac{\partial s}{\partial x_1} & \frac{\partial s}{\partial x_2} & \frac{\partial s}{\partial x_3} \\ \frac{\partial t}{\partial x_1} & \frac{\partial t}{\partial x_2} & \frac{\partial t}{\partial x_3} \end{bmatrix} \\ &= \dot{\mathbf{J}}\mathbf{J}^{-1} \end{aligned} \tag{14}$$

Since the design velocity vector, $\mathbf{V}(\mathbf{x})$, has the same interpolation with the displacement, $\dot{\mathbf{J}}$ term in the above equation can be easily calculated.

The explicitly dependent term of strain, $\varepsilon_{\mathbf{V}}(\mathbf{z})$, in (12) can be obtained from

$$\varepsilon_{\mathbf{V}}(\mathbf{z}) = -\mathbf{S}\Lambda\mathbf{G}\mathbf{d} \tag{15}$$

where

$$\mathbf{S} = \begin{bmatrix} 1&0&0&0&0&0&0&0&0 \\ 0&0&0&0&1&0&0&0&0 \\ 0&0&0&0&0&0&0&0&1 \\ 0&1&0&1&0&0&0&0&0 \\ 0&0&0&0&0&1&0&1&0 \\ 0&0&1&0&0&0&1&0&0 \end{bmatrix} \tag{16}$$

$$\Lambda = \begin{bmatrix} \nabla\mathbf{V} & \mathbf{0} & \mathbf{0} \\ \mathbf{0} & \nabla\mathbf{V} & \mathbf{0} \\ \mathbf{0} & \mathbf{0} & \nabla\mathbf{V} \end{bmatrix}_{9\times 9} \tag{17}$$

$$\mathbf{G} = \begin{bmatrix} N_{1,1}&0&0&N_{2,1}&0&0&\cdots&N_{8,1}&0&0 \\ N_{1,2}&0&0&N_{2,2}&0&0&&N_{8,2}&0&0 \\ N_{1,3}&0&0&N_{2,3}&0&0&&N_{8,3}&0&0 \\ 0&N_{1,1}&0&0&N_{2,1}&0&&0&N_{8,1}&0 \\ 0&N_{1,2}&0&0&N_{2,2}&0&&0&N_{8,2}&0 \\ 0&N_{1,3}&0&0&N_{2,3}&0&&0&N_{8,3}&0 \\ 0&0&N_{1,1}&0&0&N_{2,1}&&0&0&N_{8,1} \\ 0&0&N_{1,2}&0&0&N_{2,2}&&0&0&N_{8,2} \\ 0&0&N_{1,3}&0&0&N_{2,3}&&0&0&N_{8,3} \end{bmatrix} \tag{18}$$

The constant $\mathbf{S}$ matrix maps the second-order tensor to the vector, and $\mathbf{G}$ is the second kind of strain-displacement matrix.

Using Gauss quadrature and (3) and (15), the explicitly dependent term in (12) can be approximated as

$$a'_{\mathbf{V}}(\mathbf{z},\bar{\mathbf{z}}) \cong -\bar{\mathbf{d}}^T \left[\sum_{i=1}^{N_{\text{quad}}} w_i \left(\mathbf{G}^T \Lambda^T \mathbf{S}^T \mathbf{C}\mathbf{B}\mathbf{d} + \mathbf{B}^T \mathbf{C}\mathbf{S}\Lambda\mathbf{G}\mathbf{d} - \mathbf{B}^T \mathbf{C}\mathbf{B}\mathbf{d} div\mathbf{V} \right)_{(i)} |\mathbf{J}|_{(i)} \right] \tag{19}$$

Equation (12) is the structural fictitious load in the continuum domain, while (19) is its counterpart in the discrete domain.

4.3 Body forces

In the perturbed design, the load form for the body force can be written as

$$\ell_{\Omega_\tau} = \iiint_{\Omega_\tau} \bar{\mathbf{z}}_\tau^T \mathbf{b}_\tau d\Omega_\tau \tag{20}$$

An important idea of the continuum approach is to transform first the perturbed domain into the original domain using transformation relation: $d\Omega_\tau = |\mathbf{T}|\, d\Omega$. The material derivative of the load form in (20) then becomes

$$\ell'_{\mathbf{V}}(\bar{\mathbf{z}}) = \iiint_{\Omega} \left[\bar{\mathbf{z}}^T (\nabla \mathbf{b} \cdot \mathbf{V}) + \bar{\mathbf{z}}^T \mathbf{b} div\mathbf{V} \right] d\Omega \tag{21}$$

where $\nabla \mathbf{b} = \partial \mathbf{b} / \partial \mathbf{x}$ is the gradient matrix of the body force and $div\mathbf{V} = \nabla \cdot \mathbf{V}$. Here we assume that that the body force does not change in the fixed spatial location. If the same discretization and numerical integration are used with the discrete structural equation, the above sensitivity expression for the body force can be discretized by

$$\ell'_{\mathbf{V}}(\bar{\mathbf{z}}) \cong \bar{\mathbf{d}}^T \left[\sum_{i=1}^{N_{\text{quad}}} w_i \mathbf{N}_{(i)}^T (\nabla \mathbf{b} \cdot \mathbf{V} + \mathbf{b} div\mathbf{V})_{(i)} \left| \mathbf{J}_{(i)} \right| \right] \tag{22}$$

4.4 Surface traction–pressure load

For simplicity of comparison, we only consider the pressure load that applies to the normal direction to the surface; i.e., $\mathbf{t} = p\mathbf{n}$. In the perturbed design, the load linear form for the surface traction can be written as

$$\ell_{\Omega_\tau}(\bar{\mathbf{z}}) = \iint_{\Gamma_{s_\tau}} \bar{\mathbf{z}}_\tau^T (p_\tau \mathbf{n}_\tau)\, d\Gamma_\tau \tag{23}$$

In the material derivative of the above load linear form, we use the property that the pressure does not change in the fixed spatial coordinate. However, the normal direction and the area of the surface can be changed according to the shape design variables. In order to simplify the presentation, the material derivative of the infinitesimal surface element is derived first. Consider an infinitesimal surface element in the perturbed design (see Fig. 4) as

$$\mathbf{n}_\tau d\Gamma_\tau = |\mathbf{T}|\, \mathbf{T}^{-T} \mathbf{n} d\Gamma \tag{24}$$

where $\mathbf{T}$ is the Jacobian matrix between the initial and perturbed design. Since only $\mathbf{T}$ depends on the design in the above expression and $\mathbf{T} = \mathbf{I}$ when $\tau = 0$, the material derivative of this surface element becomes (Choi and Kim 2004)

$$\begin{aligned} \frac{d}{d\tau} \left[\mathbf{n}_\tau d\Gamma_\tau \right] \Big|_{\tau=0} &= \frac{d}{d\tau} \left(|\mathbf{T}| \right) \mathbf{n} d\Gamma + \frac{d}{d\tau} \left(\mathbf{T}^{-T} \right) \mathbf{n} d\Gamma \\ &= (div\mathbf{V})\, \mathbf{n} d\Gamma - \nabla \mathbf{V}^T \mathbf{n} d\Gamma \end{aligned} \tag{25}$$

Using (25), the material derivative of (23) becomes

$$\ell'_{\mathbf{V}}(\bar{\mathbf{z}}) = \iint_{\Gamma_s} \bar{\mathbf{z}}^T \left[(\nabla p^T \mathbf{V}) \mathbf{I} + (p div\mathbf{V})\, \mathbf{I} - p \nabla \mathbf{V}^T \right] \mathbf{n}\, d\Gamma \tag{26}$$

Before discretization of the above sensitivity expression, we need to introduce a transformation between the physical surface and the surface in the reference domain because the surface traction is applied in the normal direction to the boundary of the domain (see Fig. 4). An infinitesimal surface area with unit normal vector can be transformed into the reference domain as

$$\mathbf{n} d\Gamma = \frac{\partial \mathbf{x}}{\partial r} dr \times \frac{\partial \mathbf{x}}{\partial s} ds = |\mathbf{J}|\, \mathbf{J}^{-T} \cdot \mathbf{k} dr ds \tag{27}$$

where $\mathbf{k} = [0, 0, 1]^T$ is a unit vector, and r and s are two coordinate directions in the reference domain. By substituting (27) into (26) and by applying numerical

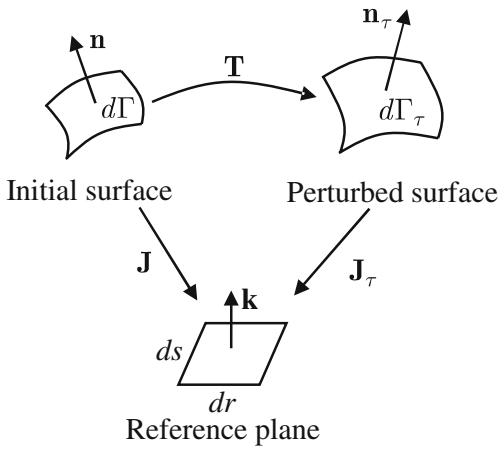

Fig. 4 Infinitesimal surface element in the initial and perturbed domain

integration, the above sensitivity expression for the surface traction can be discretized by

$$\ell'_{\mathbf{V}}(\bar{\mathbf{z}}) \cong \bar{\mathbf{d}}^T \left[\sum_{i=1}^{N_{\text{quad}}} w_i \mathbf{N}_{(i)}^T \left\{ (\nabla p^T \mathbf{V})\mathbf{I} + (p div \mathbf{V})\,\mathbf{I} - p \nabla \mathbf{V}^T \right\}_{(i)} \left(|\mathbf{J}|\,\mathbf{J}^{-T} \cdot \mathbf{k} \right)_{(i)} \right] \tag{28}$$

5 Shape design sensitivity equations—discrete derivatives

In the discrete approach, the design sensitivity equation is obtained by taking the derivative of the discrete system of equations. A key idea here is that the differentiation takes place between discretization and numerical integration. If the differentiation occurs after numerical integration, it is called the semi-analytical method in which finite different derivative is used to approximate the derivatives of stiffness matrix and load vector.

5.1 Stiffness part

For the stiffness part, we differentiate (4) to obtain

$$\left(\bar{\mathbf{d}}^T \mathbf{K} \mathbf{d} \right)' = \bar{\mathbf{d}}^T \mathbf{K} \dot{\mathbf{d}} + \bar{\mathbf{d}}^T \mathbf{K}' \mathbf{d} \tag{29}$$

where the first term on the right-hand side is the implicitly dependent term through the nodal displacements, while the second term is the explicitly dependent term through the stiffness matrix, whose expression for a single element can be obtained as

$$\bar{\mathbf{d}}^T \mathbf{K}' \mathbf{d} = \bar{\mathbf{d}}^T \sum_{i=1}^{N_{\text{quad}}} w_i \left[\left(\dot{\mathbf{B}}^T \mathbf{C} \mathbf{B} \mathbf{d} + \mathbf{B}^T \mathbf{C} \dot{\mathbf{B}} \mathbf{d} \right)_{(i)} |\mathbf{J}_{(i)}| + \left(\mathbf{B}^T \mathbf{C} \mathbf{B} \mathbf{d} \right) |\mathbf{J}_{(i)}|^{\bullet} \right] \tag{30}$$

Since the strain–displacement matrix is composed of the derivative of the shape functions, which is independent of shape design, and the inverse of the Jacobian matrix, the core of the above expression is the material derivative of the Jacobian matrix and its determinant. Indeed from the material derivative formula in Choi and Kim (2004), it has been shown that

$$\frac{d}{d\tau} |\mathbf{J}_\tau| \Big|_{\tau=0} = div \mathbf{V}\, |\mathbf{J}| \tag{31}$$

$$\frac{d}{d\tau} \mathbf{J}_\tau^{-1} \Big|_{\tau=0} = -\mathbf{J}^{-1} \cdot \nabla \mathbf{V} \tag{32}$$

Using (32), it is possible to show that the derivative of the strain–displacement matrix becomes $\dot{\mathbf{B}} = -\mathbf{S}\boldsymbol{\Lambda}\mathbf{G}$. Thus, by substituting this relation and (31) into (30), we can obtain the explicitly dependent term in the discrete approach as

$$\bar{\mathbf{d}}^T \mathbf{K}' \mathbf{d} = -\bar{\mathbf{d}}^T \left[\sum_{i=1}^{N_{\text{quad}}} w_i \left(\mathbf{G}^T \boldsymbol{\Lambda}^T \mathbf{S}^T \mathbf{C} \mathbf{B} \mathbf{d} + \mathbf{B}^T \mathbf{C} \mathbf{S} \boldsymbol{\Lambda} \mathbf{G} \mathbf{d} - \mathbf{B}^T \mathbf{C} \mathbf{B} \mathbf{d} div \mathbf{V} \right)_{(i)} |\mathbf{J}_{(i)}| \right] \tag{33}$$

which is identical with the continuum form after discretization in (19). In the following subsection, we will show that the same is true for the load forms.

The derivative of the applied load, $\mathbf{F}'$, will be presented in the following subsection. Then, the discrete design sensitivity equation is obtained as

$$\mathbf{K}\mathbf{d} = \mathbf{F}' - \mathbf{K}'\mathbf{d} \tag{34}$$

5.2 Body forces

After discretization and numerical integration, the load linear form corresponding to the body force can be written as

$$\ell_\Omega(\bar{\mathbf{z}}) \cong \bar{\mathbf{d}}^T \mathbf{F}_b \tag{35}$$

where

$$\mathbf{F}_b = \sum_{i=1}^{N_{\text{quad}}} w_i \mathbf{N}_{(i)}^T \mathbf{b}_{(i)} |\mathbf{J}_{(i)}| \tag{36}$$

In the discrete sensitivity formulation, the discrete force in (36) is differentiated with respect to the design. Since the shape function is defined in the reference element, it is independent of shape design. Thus, it is only necessary to differentiate the body force and the determinant of Jacobian. The derivative of the discrete body force becomes

$$\mathbf{F}'_b = \sum_{i=1}^{N_{\text{quad}}} w_i \mathbf{N}_{(i)}^T \left(\nabla \mathbf{b}_{(i)} \mathbf{V} |\mathbf{J}_{(i)}| + \mathbf{b}_{(i)} |\mathbf{J}_{(i)}|^{\bullet} \right) \tag{37}$$

In the above equation, we use the property of $\mathbf{b}' = 0$ It is also possible to show that $|\mathbf{J}|^{\bullet} = div \mathbf{V}\, |\mathbf{J}|$. Then, by comparing (22) and (37), the sensitivity expressions of the body force are identical for the continuum and discrete methods if the same discretization and numerical integration are used.

5.3 Surface traction–pressure load

After discretization and numerical integration, the load linear form corresponding to the surface traction can be written as

$$\ell_{\Omega}(\bar{\mathbf{z}}) \cong \bar{\mathbf{d}}^{T}\mathbf{F}_{s} \tag{38}$$

where

$$\mathbf{F}_{s} = \sum_{i=1}^{N_{\text{quad}}} w_i \mathbf{N}_{(i)}^{T} \left(p\,|\mathbf{J}|\,\mathbf{J}^{-T}\cdot\mathbf{k}\right)_{(i)} \tag{39}$$

The above pressure load can be differentiated to obtain the following sensitivity expression:

$$\mathbf{F}'_{s} = \sum_{i=1}^{N_{\text{quad}}} w_i \mathbf{N}_{(i)}^{T}\Big(\left(\nabla p^{T}\mathbf{V}\right)|\mathbf{J}|\,\mathbf{J}^{-T}\cdot\mathbf{k} + p\,|\mathbf{J}|^{\bullet}\,\mathbf{J}^{-T} \cdot\mathbf{k} + p\,|\mathbf{J}|\left(\mathbf{J}^{-T}\right)^{\bullet}\cdot\mathbf{k}\Big)_{(i)} \tag{40}$$

where we use the property of $p' = 0$. Now we can use the property of $|\mathbf{J}|^{\bullet} = |\mathbf{J}|\,div\mathbf{V}$ and $\left(\mathbf{J}^{-T}\right)^{\bullet} = \nabla\mathbf{V}^{T}\cdot\mathbf{J}^{-T}$ to yield

$$\mathbf{F}'_{s} = \sum_{i=1}^{N_{\text{quad}}} w_i \mathbf{N}_{(i)}^{T}\Big[\left(\nabla p^{T}\mathbf{V}\right)\mathbf{I} + (p\,div\mathbf{V})\,\mathbf{I} + p\nabla\mathbf{V}^{T}\Big]_{(i)} \times \left(|\mathbf{J}|\,\mathbf{J}^{-T}\cdot\mathbf{k}\right)_{(i)} \tag{41}$$

It is obvious that (41) is identical with the expression in (28).

So far, we have shown that the discrete sensitivity expressions from both continuum discrete approaches are identical. However, this conclusion is based on the fact that both approaches use the same discretization, numerical integration, and the same discrete linear design velocity vector. This is somewhat different from the observation by Choi and Twu (1988) in which additional requirements are suggested, such as exact integration and exact solution.

6 Numerical examples

In this section we present two numerical examples. The purpose of the first example is to show that the sensitivity results may be consistent with the numerical solution, but it can be different from the analytical one because the numerical solution has errors associated with approximation. The second example demonstrates the use of the sensitivity calculation with body force and surface traction loading simultaneously in shape optimization.

6.1 Cantilever beam under uniform pressure load

Consider a cantilevered beam under uniform pressure as shown in Fig. 5. The following geometric and material properties are used: $L = 5$ m, $b = 0.25$ m, $h = 0.4$ m, $q = 10$ kN/m^2, $E = 20$ GPa, and $v = 0.2$. From the classical beam theory, the displacement of the tip is given as

$$w_{\text{tip}} = -\frac{qL^4}{8EI} = -\frac{3qL^4}{2Ebh^3} \tag{42}$$

The shape of the beam is related to the length and height of the beam. By differentiating the above equation with respect to these two shape parameters, analytical sensitivities can be obtained as

$$\frac{\partial w_{\text{tip}}}{\partial L} = -\frac{6qL^3}{Ebh^3} \tag{43}$$

$$\frac{\partial w_{\text{tip}}}{\partial h} = \frac{9qL^4}{2Ebh^4} \tag{44}$$

For numerical solution, the beam structure is discretized using 240 eight-node hexahedral elements (see Fig. 5). For structural analysis the EFEAPpv (Extended Finite Element Analysis Program for Personal Version) (Zienkiewicz and Taylor 2005) is used. Figure 6 shows the transverse displacement from analytical solution and finite element solution. Due to approximation errors, the finite element solution is stiffer than the analytical one.

For the purpose of comparison, sensitivity results are presented using three methods: sensitivity from global

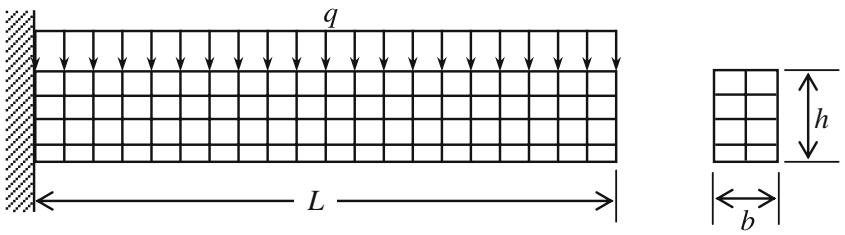

Fig. 5 Cantilevered beam under uniform pressure load

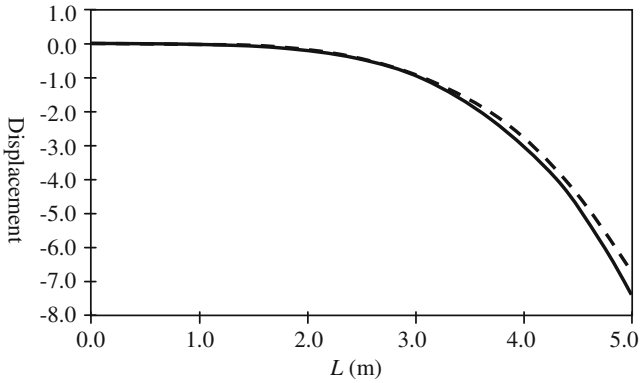

Fig. 6 Transverse displacements; *solid line* analytical solution, *dashed line* finite element solution

finite difference, sensitivity of discrete solution, and the sensitivity of continuous solution from (43) and (44). After a series of trial-and-errors, a perturbation size of 0.001 is selected for the global finite difference. Since both the continuum and discrete approaches are identical, only one method is presented in the name of sensitivity of discrete solution. Tables 1 and 2 show the transverse displacement sensitivity with respect to beam length and height, respectively. It is noted that the sensitivity results from global finite difference and continuum approach are almost identical. This agreement will depends on perturbation size in finite difference calculation. Nonlinear effect will cause error for large perturbation size, whereas numerical noise will be dominated for too small perturbation size. This has been a major bottleneck of finite difference-based sensitivity calculation.

It is also noted that both sensitivity results are different from the sensitivity of continuous solution obtained from (43) and (44). The errors in sensitivity

Table 1 Transverse displacement sensitivity with respect to beam length

L (m)	Finite difference sensitivity	Sensitivity of discrete solution	Sensitivity of continuous solution
0.00	0.000E+00	0.000E+00	0.000E+00
0.50	−7.506E−07	−7.506E−07	−5.859E−06
1.00	−4.960E−05	−4.960E−05	−4.688E−05
1.50	−1.603E−04	−1.603E−04	−1.582E−04
2.00	−3.721E−04	−3.721E−04	−3.750E−04
2.50	−7.152E−04	−7.153E−04	−7.324E−04
3.00	−1.218E−03	−1.218E−03	−1.266E−03
3.50	−1.904E−03	−1.904E−03	−2.010E−03
4.00	−2.794E−03	−2.795E−03	−3.000E−03
4.50	−3.909E−03	−3.910E−03	−4.271E−03
5.00	−5.257E−03	−5.258E−03	−5.859E−03

Table 2 Transverse displacement sensitivity with respect to beam height

h (m)	Finite difference sensitivity	Sensitivity of discrete solution	Sensitivity of continuous solution
0.150	1.402E+00	1.402E+00	2.778E+00
0.200	5.733E−01	5.734E−01	8.789E−01
0.250	2.694E−01	2.695E−01	3.600E−01
0.300	1.409E−01	1.409E−01	1.736E−01
0.350	8.040E−02	8.043E−02	9.371E−02
0.400	4.858E−02	4.860E−02	5.493E−02

results are caused by discretization. Finite difference and discrete–discrete sensitivities are obtained by differentiating this erroneous discrete equation. On the other hand, the continuum–discrete sensitivity also has an error because the analytical sensitivity equation is solved through discretization. If the continuum sensitivity equation is analytically solved, then the sensitivity results will be identical to the exact one (last column) of the two Table. This leads to the conclusion that the continuum–discrete and discrete–discrete sensitivity results are consistent with the numerical solution, but that does not mean that the obtained sensitivity results are exact. They are obtained with the inherent errors in the numerical solution. The effect of these errors is magnified when the thickness of the beam is small.

6.2 Shape optimization of an arch dam

Consider a crown cantilever of an arch dam as shown in Fig. 7. For the crown cantilever of a double-curvature

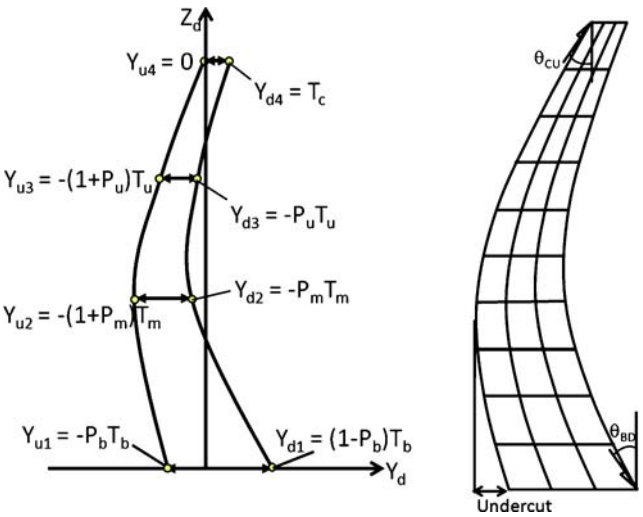

Fig. 7 The profile of crown cantilever and the finite element mesh at the initial design

arch dam, as shown in Fig. 7, a polynomial of mth-order (usually $m = 2$ or 3) is used to determine the curve of the upstream face and another polynomial is used to determine the thickness. In this paper, the crown shape is defined using Hermit splines (Ahmadi and Pahl 2003). For the fixed four vertical locations in Fig. 7, the horizontal locations of four reference points of up- and down-stream are as follows

$$\begin{aligned} Y_{u1} &= -P_b\, T_b & Y_{d1} &= (1 - P_b)\, T_b \\ Y_{u2} &= -(1 + P_m)\, T_m & Y_{d2} &= -P_m T_m \\ Y_{u3} &= -(1 + P_u)\, T_u & Y_{d3} &= -P_u T_u \\ Y_{u4} &= 0 & Y_{d4} &= T_c \end{aligned} \tag{45}$$

where Y_{ui}, Y_{di} are upstream and downstream interpolation node coordinates, respectively. Thickness of the crown cantilever at desired level Z is obtained from the following equation:

$$\begin{aligned} T(z) &= Y_d - Y_u \\ &= \text{Spline}(Y_{di}, H_i, Z) - \text{Spline}(Y_{ui}, H_i, Z) \end{aligned} \tag{46}$$

For this shape, design variables are the crown thicknesses (T_b, T_m, T_u, T_c) and the overhang parameters (p_b, p_m, p_u) at the interpolation stations (see Fig. 7). For design sensitivity analysis, the values of the initial design variables are summarized in Table 3.

Two loadings are considered in the process of shape sensitivity analysis: (1) body force due to gravity and (2) surface traction due to the hydrostatic pressure (with full reservoir). The pressure load has triangular distribution along the height of the cantilever. For design sensitivity analysis and optimization purpose, hydrostatic and gravity loads are simultaneously applied to the finite element model. The following material properties of the arch dam are used: Young's modulus $E = 21$ GPa, Poisson's ratio $\nu = 0.25$, and specific weight $\gamma_c = 24{,}000\ \text{N/m}^3$.

Design sensitivities of displacements and principal stresses are plotted in Figs. 8 and 9. In Fig. 8, both the vertical and lateral displacement sensitivities are matched well with those from the finite difference method. Sensitivity results are presented along the height of the cantilever at the middle layer. A perturbation size of $\Delta x = 0.005$ is used for the finite difference sensitivity.

Table 3 Initial values of shape design variables

H_c(m)	T_c(m)	T_u(m)	T_m(m)	T_b(m)	P_u	P_m	P_b
80	10	20	34	50	.05	0.10	0.7

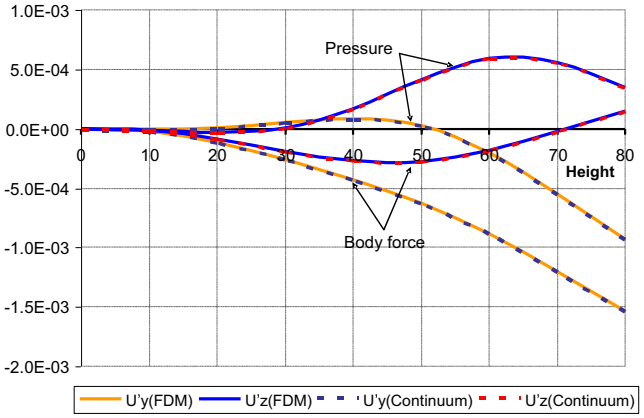

Fig. 8 Displacements sensitivity of body force and pressure load w.r.t T_u

The nonlinear constrained optimization problem for the arch dam structure for a existing dam with above material properties and $H_c = 100$ (m) can be written with seven design variables, $\mathbf{x} = \{T_c, T_u, T_m, T_b, P_u, P_m, P_b\}$, as

$$\begin{aligned} &\text{Minimize Area} = f(\mathbf{x}) \\ &\text{Subject to } \theta_{CU} \le 16.5^\circ \\ &\qquad \theta_{BD} \le 25^\circ \\ &\qquad \text{Undercut}(\mathbf{x}) \le 6.0 \\ &\qquad y_u'' \ge 0 \\ &\qquad T_c(\mathbf{x}) \ge 6.0 \\ &\qquad \sigma_t(\mathbf{x}) \le 10.0\,\text{MPa} \\ &\qquad \sigma_c(\mathbf{x}) \le 100.0\,\text{MPa} \end{aligned} \tag{47}$$

where

$$f(x) = \frac{1}{4} H_{dam}\,(.5T_c + 1.2T_u + 1.5T_m + .8T_b) \tag{48}$$

$$S_c = \frac{-\frac{175}{1{,}342}Y_{u1} + \frac{8{,}625}{9{,}394}Y_{u2} - \frac{26{,}688}{4{,}697}Y_{u3} + \frac{3{,}284}{671}Y_{u4}}{H_{dam}} \tag{49}$$

$$S_b = \frac{H_{dam}}{-\frac{4,315}{1{,}342}Y_{d1} + \frac{40{,}125}{9{,}394}Y_{d2} + \frac{6{,}528}{4,697}Y_{d3} + \frac{224}{671}Y_{d4}} \tag{50}$$

$$\text{Undercut} = Y_{u1} - Y_{\text{zero}} \tag{51}$$

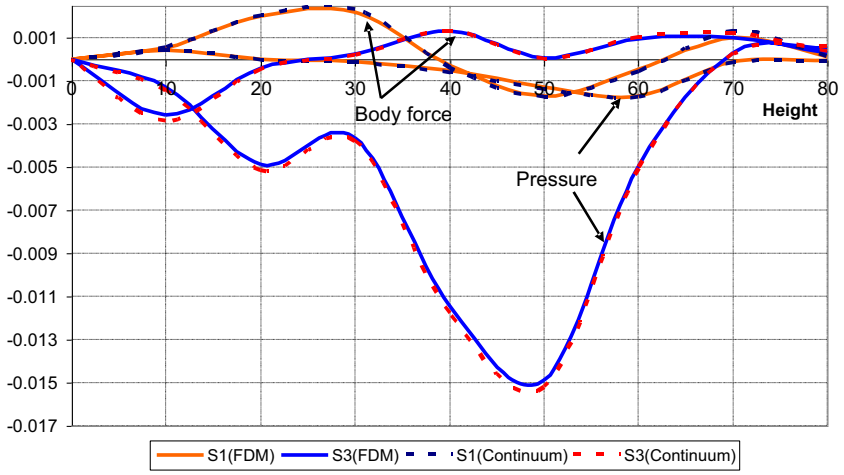

Fig. 9 Principles stress sensitivity of body force and pressure load w.r.t T_u

with Y_{zero} being a point at the upstream face in which the slope is zero and y''_u is the curvature of upstream face at $z = 0.75H$.

A sequential quadratic programming (SQP) algorithm is used to solve the optimization problem in (47). Except for stress constraints, the objective function

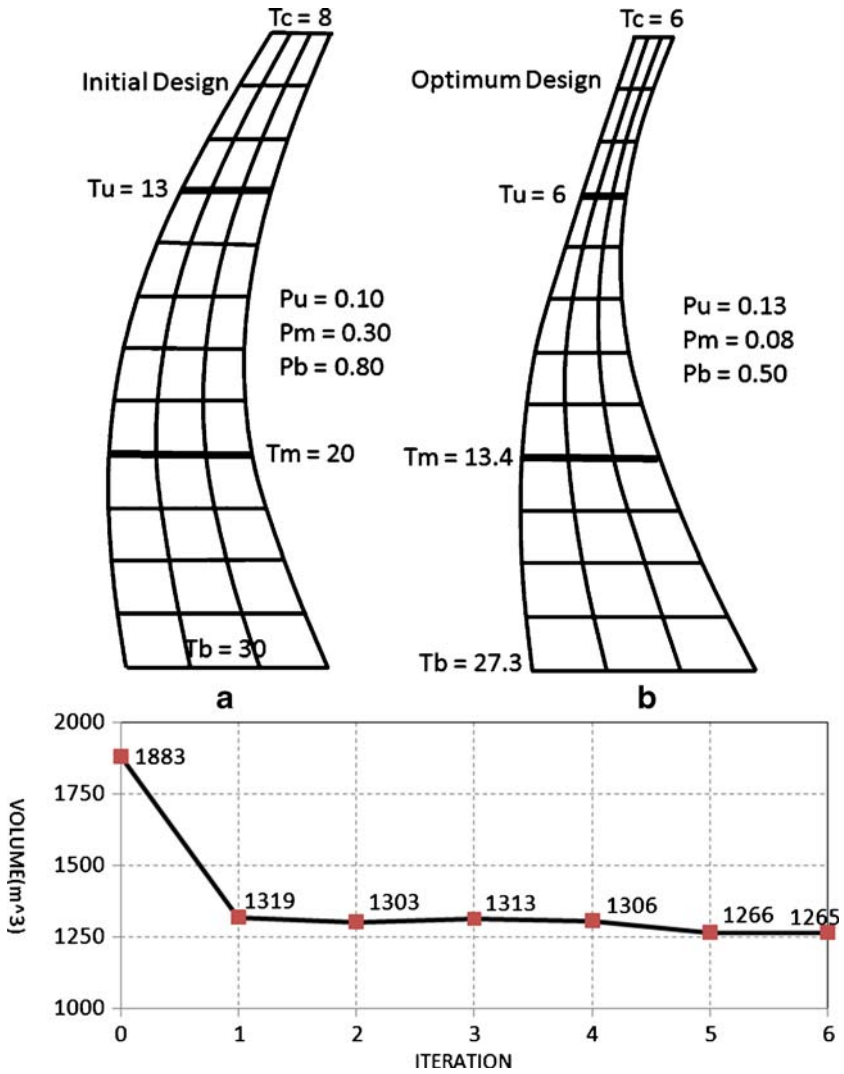

Fig. 10 Initial and optimum shape of arch dam cantilever and history of cost function

and other constraints are explicit function of design variables. Thus, it is trivial to calculate analytical sensitivity. The sensitivity of stress constraints are calculated using the displacement sensitivity and the chain rule of differentiation.

The optimization problem is converged after six iterations. Since the initial design is conservative, most design variables are reduced. The optimum design reduces the area of the structure by 35%. However, this reduction depends on how the initial design was selected. Figure 10 shows the shape of the arch dam cantilever at the initial and optimum designs and history of objective function.

7 Conclusions and discussions

In this paper, we presented shape sensitivity formulations for structures under design-dependent loadings, such as body forces and surface tractions. It is shown that the discrete and continuum approaches are identical in the discrete level when the same discretization, numerical integration, and linear design velocity fields are used. These requirements are more flexible than the previous observation by Choi and Twu (1988) in which the exact integration and exact analytical solutions are required. It is also shown that the numerically calculated sensitivity results may be consistent with the finite difference sensitivity results, but they can be different from the analytical sensitivities because of approximation error.

References

Ahmadi MT, Pahl PJ (2003) A research proposal for design optimization of concrete arch dams for enhanced seismic response. Tarbiat Modares University and Technical Berlin University

Arora JS (1993) An exposition of the material derivative approach for structural shape sensitivity analysis. Comput Methods Appl Mech Eng 105:41–62

Arora JS, Lee TH, Cardoso JB (1992) Structural shape sensitivity analysis: relationship between material derivative and control volume approaches. AIAA J 36:1638–1648

Choi KK, Haug EJ (1983) Shape design sensitivity analysis of elastic structures. J Struct Mech 11(2):231–269

Choi KK, Kim NH (2004) Structural sensitivity analysis and optimization: linear systems, vol 1. Springer, New York

Choi KK, Twu S-L (1988) On equivalence of continuum and discrete methods of shape sensitivity analysis. AIAA J 27(10):1418–1424

Haftka RT, Adelman HM (1989) Recent developments in structural sensitivity analysis. Struct Optim 1:137–151

Haftka RT, Grandhi RV (1986) Structural shape optimization—a survey. Comput Methods Appl Mech Eng 57:91–106

Hardee E, Chang K-H, Tu J, Choi KK, Grindeanu I, Yu X (1999) A CAD-based design parameterization of elastic solids. Adv Eng Softw 30:185–199

Haug EJ, Choi KK, Komkov V (1985) Design sensitivity analysis of structural systems. Academic, Orlando, FL

Hughes TJR (1987) The finite element method: linear static and dynamic finite element analysis. Prentice-Hall, Englewood Cliffs, NJ

Kim NH, Choi KK, Botkin M (2003) Numerical method for shape optimization using meshfree method. Struct Multidiscipl Optim 24(6):418–429

Kwak BM (1994) A review on shape optimal design and sensitivity analysis. Struct Eng/Earthqu Eng 10(4):159s–174s

Mota Soares CA, Rodrigues HC, Choi KK (1984) Shape optimal structural design using boundary elements and minimum compliance techniques. J Mech Transm Autom Des 106: 518–523

Santos JLT, Choi KK (1989) Integrated computational considerations for large scale structural design sensitivity analysis and optimization. In: Eschenauer HA, Thierauf G (eds) Discretization methods and structural optimization—procedures and applications. Springer, Berlin, pp 299–307

van Keulen F, Haftka RT, Kim NH (2005) Review of options for structural design sensitivity analysis, part1: linear systems. Comput Methods Appl Mech Eng 194(30–33):3213–3243

Yang RJ, Botkin ME (1986) The relationship between the variational approach and the implicit differentiation approach to shape design sensitivities. In: Bennett JA, Botkin ME (eds) The optimum shape: automated structural design. Plenum, New York, pp 61–77

Zienkiewicz OC, Taylor RL (2005) The finite element method, 6th edn. Elsevier, Oxford